Geosynthetics: Applications, Design and Construction, De Groot, Den Hoedt & Termaat (eds)
© 1996 Balkema, Rotterdam. ISBN 90 5410 836 3

Deformation behavior of geotextile reinforcement at vicinity of shear surface

D.T. Bergado & P.V. Long
School of Civil Engineering, Asian Institute of Technology (AIT), Bangkok, Thailand
G. Werner
Polyfelt Ges.m.b.H., Linz, Austria

ABSTRACT: Large direct shear model tests and finite element method (FEM) have been conducted for investigating the deformation behavior of geotextile reinforcement at vicinity of shear surface. A series of large direct shear tests across the reinforcement have been performed. Nonwoven, needle-punched geotextiles having nominal mass of 130 g/m^2 and 280 g/m^2 have been examined. The reinforcement were confined in silty sand at different normal stresses. The displacements of the reinforcement and surrounding soil at the vicinity of shear surface have been measured using wire extensometers connected to LVDTs. The mobilization of strain and orientation of the reinforcement have been presented as functions of shear displacement. The test results indicated that the mobilized strain in geotextile decreased with increasing of geotextile stiffness and slightly increased with increasing of confining stress. The mobilized orientation of reinforcement force seems independent of the geotextile stiffness. The limiting strain of the geotextile reinforcements at equilibrium state considering strain compatibility has been discussed. The test method presented herein may be a realistic approach for determining the magnitude and orientation of the mobilized reinforcement force that is necessary in stability analysis of geotextile reinforced earth structures. The test results have also been interpreted using FEM.

1. INTRODUCTION

Geotextiles are being increasingly employed in the design and construction of embankment over soft clays. It has been found to be technically feasible, operationally practical and cost-effective alternative to conventional construction methods. There are some validated rational design methods available for selection of geotextiles as reinforcement or for evaluating the effect of this reinforcement upon embankment behavior. Limit equilibrium analyses with circular slip surfaces have been commonly used in conventional design of geotextile reinforced embankments on soft ground. In this method, two important factors have to be considered, namely: (i) the mobilized tensile strain, ε_{mob}, in the geotextile near the vicinity of the shear surface at the limit equilibrium state which will dictate the magnitude of the mobilized tensile force, and (ii) the orientation of the geotextile tensile force which is represented by the inclination factor, I_f. In practical design, however, these factors have often been selected arbitrarily. The mobilized tensile strain may be taken from 2 to 10 % depending on the behavior of foundation soil (Bonaparte and Christopher, 1987). The values of I_f ranges from 0 to 1 corresponding to horizontal and tangential direction of the reinforcement tensile force, respectively. The tensile force has been considered to act horizontally by Fowler (1982) and Jewell (1982), tangentially by Quast (1983) and Delmas et al. (1992) as well as between tangential and horizontal (bisector) direction (Bonaparte and Christopher, 1987; Huisman, 1987). In this study, the mobilized strain and orientation of geotextile reinforcement caused by the localized deformation of confining soil associated with the development of a shear surface have been investigated by large direct shear model tests together with finite element analyses (FEM).

2. TEST SETUP AND INSTRUMENTATION

This study involves the use of low-strength, nonwoven needle-punched geotextile, namely: TS420 and TS700, having nominal mass of 130 g/m^2 and 280 g/m^2, and ultimate strength of 8 kN/m and 18 kN/m, respectively. The silty sand that has been widely used in construction of highway embankments in Bangkok Plain was employed as backfill material.

The tests were conducted in large direct shear box which was made of 9.5 mm thick steel plate with an inside dimension of 930 mm in length by 580 mm in width by 560 mm in height facilitates the shear surface of $0.54 m^2$. The compaction was done with 150 mm lift at moisture content of 13 % and dry density of 17 kN/m^3 corresponding to 95 % standard Proctor. Then, the compacted backfill soil was cut to the desired inclination angle of 60^0 from the horizontal surface. Subsequently, the geotextile specimen having dimension of 580 mm in width by 1000 mm in length was located in place as seen in Fig. 1. Finally, the geotextile was covered with soil compacted in lifts. The normal stress was applied by pressurized air bag. The shear force was applied by a 225 kN capacity electro-hydraulic controlled jack and was measured by an electrical load cell. The rate of shearing was kept at 2 mm per minute throughout the tests. The displacements were measured by means of Linear Variable Differential Transformer (LVDT). The locations of displacement measurement are schematically shown in Fig. 1. A total of five LVDTs have been used: one for displacement of shear box, two for geotextile displacements (points G_1 and G_2) and two for soil at soil-geotextile interface surface (points O and B). The LVDTs were connected to the measured points by high-strength, flexible wires which were attached to geotextile and soil by rivet and L-shape aluminum anchor, respectively. Both load cell and LVDTs were connected to an Automatic Data Acquisition (ADA) system using the 21X Micro Datalogger. After each test, the orientation of geotextile was determined by digging out the backfill soil and plotting the new position of the interface surface between geotextile and backfill soil.

3. INTERPRETATION OF TEST RESULTS

Mobilized strain in geotextile

The mobilized strain in geotextile reinforcement near the shear surface can be calculated from the displacement of the reinforcement measured at locations G_1 and G_2 in Fig. 1 as follows:

$$\varepsilon = \frac{d_1 - d_2}{l_{12}} \tag{1}$$

where d_1, d_2 are the measured displacements of geotextile at points G_1 and G_2, respectively, and l_{12} is the original distance between these points. The value of l_{12} of 50 mm was set for all tests.

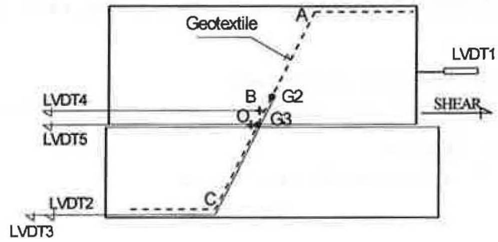

Fig. 1 Instrumentation for Large Direct Shear Tests

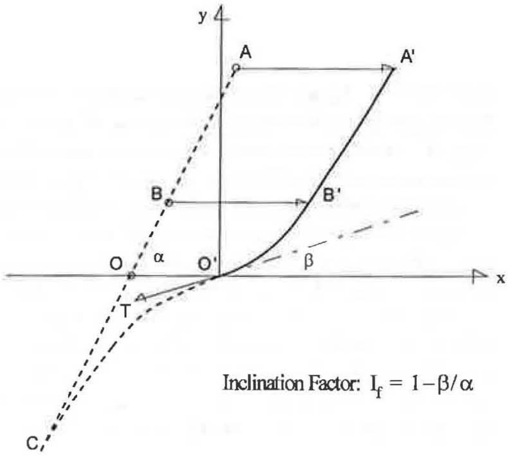

Fig. 2 Diagram for Calculating Inclination Factor

Inclination factor of geotextile

The inclination factor of geotextile reinforcement is expressed by following equation:

$$I_f = 1 - \frac{\beta}{\alpha} \tag{2}$$

where α and β, respectively, are the original and current inclination angles of the geotextile as seen in Fig. 2.

From Fig. 2, under shear displacement u, the interface surface between geotextile and backfill soil OBA moved to O'B'A'. For estimating the value of β corresponding to current shear displacement, u, the following assumptions have been made: i) the current interface surface O'B'A' is approximated by a parabola, $y = ax^2 + bx + c$, and ii) the vertical displacement of points O, B, and A can be neglected. For the purpose of estimating the curvature at point O, the first assumption may be reliable if point B is located in the highly deformed zone. The second assumption is acceptable because the vertical displacement is small comparing to the horizontal displacement. From these assumptions, the followings can be derived:

$$\tan\beta = \frac{y_A x_{B'}^2 - y_B x_{A'}^2}{x_{A'} x_{B'}^2 - x_{B'} x_{A'}^2} \quad (3)$$

where y_A and y_B are the vertical coordinates of points A and B as illustrated in Fig. 2. The others are given as follows:

$$x_A = u_A - u_O + y_A \cot\alpha \quad (4)$$

$$x_B = u_B - u_O + y_B \cot\alpha \quad (5)$$

$$u_A = AA', \quad u_B = BB' \quad \text{and} \quad u_O = OO' \quad (6)$$

In Eq. (6), AA', BB' and OO' are horizontal displacements of points A, B and O, respectively, that are measured by LVDT as described previously. The values of β obtained from Eq. (3) have also been verified by the direct measurement after digging out the soil at the end of each test.

Shear force vs shear displacement

The shear force per unit width of shear box versus shear displacement curves for sand reinforced by geotextile TS420 and TS700 are presented in Fig. 3 and 4, respectively. The results from dummy tests without reinforcements are also plotted in these figures as dotted lines for comparison. The test results indicated the peak load carrying capacity of geotextile reinforced soil. Both types of geotextile yielded significant enhancements in shear strength of reinforced specimen. The shear resistance contributed by the geotextile reinforcement have been found to be proportional to the ultimate strength of reinforcement.

Geotextile strain vs shear displacement

The local strains mobilized in geotextile at the location near the shear surface are plotted as functions of shear displacement in Fig. 5 and Fig. 6 for geotextiles TS420 and TS700, respectively. From these figures, it can be seen that the mobilized strain in geotextile increased with the decrease of geotextile stiffness, for the same shear displacement. Corresponding to the shear displacement at peak strength of unreinforced soil, the mobilized strains in geotextiles are in the order of 5 % to 10 %.

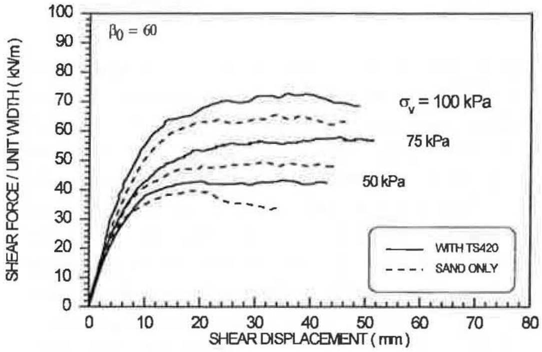

Fig. 3 Measured Shear Force-Shear Displacement Curves for Silty Sand Reinforced by TS420

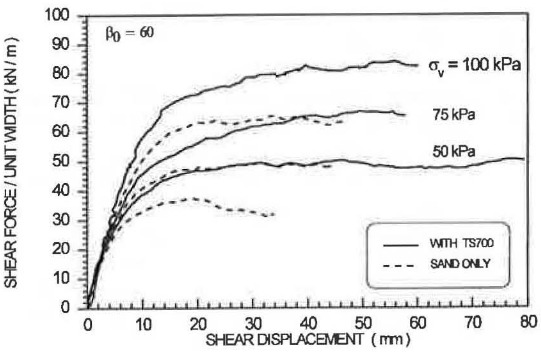

Fig. 4 Measured Shear Force-Shear Displacement Curves for Silty Sand Reinforced by TS700

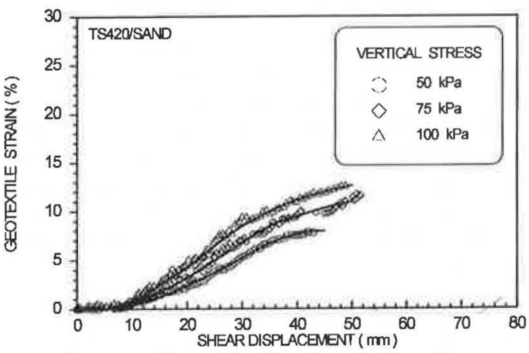

Fig. 5 Geotextile Strain vs Shear Displacement for Geotextile TS420

Inclination factor vs shear displacement

The values of inclination factor, I_f, interpreted by Equation (3) are presented as functions of shear displacement in Figs. 7 and 8 for geotextiles TS420 and TS700, respectively. The values determined by direct measurements after excavation of soil at the end of tests agreed well with the interpreted results as seen in the aforementioned figures. The test results indicated that the orientation of geotextile reinforcement cannot attain the tangential direction of shear surface even at large shear displacement corresponding to residual strength of soil. The values of inclination factor at shear displacement corresponding to the peak strength of unreinforced soil are in the order of 0.25 to 0.50. The inclination factor seemed independent on the geotextile stiffness and the applied vertical stress as well.

Finite element analysis

Finite element analyses using PLAXIS program (Vermeer & Brinkgreve, 1995) have been carried out for verification of the test results and back calculation of the soil-geotextile interaction behavior. The soil specimen are modelled by twenty-eight 15-noded triangular elements. The slippage between soil and geotextile reinforcement is considered by using 10-noded interface elements. The Mohr-Coulomb's elastic perfectly plastic model is used for both backfill soil and soil-geotextile interface. The 5-noded bar elements using elastic stress-strain relation is employed for the geotextile reinforcement. The shearing process is simulated by applying the prescribed displacements at the boundaries of the upper half of the shear box. The friction angle, $\phi' = 30^0$, and cohesion, c' = 10 kPa, as given from the large direct shear test results are used for soil. The shear modulus of soil and the stiffness of geotextile are obtained by back analyzing the measured data.

The FEM results are given in Figs. 9 to 12. The field of displacement vectors is shown in Fig. 9. Also seen from this figure is the deformation of the geotextile reinforcement. The principle stress field are illustrated in Figs. 10a and 10b for unreinforced and reinforced samples, respectively. Good agreements between the calculated and measured results can be seen in Figs. 11 and 12 for shearing of soil only and soil reinforced by geotextile, respectively. Moreover, the FEM back-analyzed results indicated that the interface strength ratio, defined as the ratio of shear strength at soil-geotextile interface to the shear strength of soil only, is equal to 1.

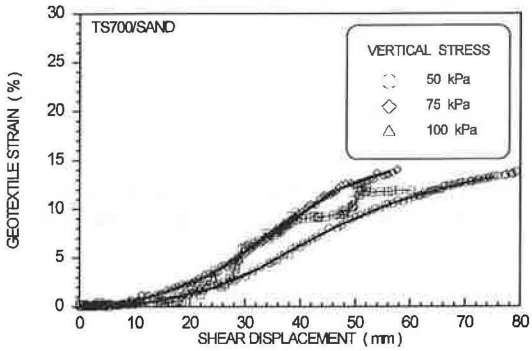

Fig. 6 Geotextile Strain vs Shear Displacement for Geotextile TS700

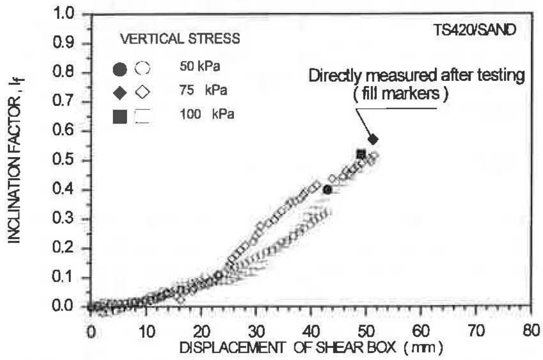

Fig. 7 Inclination Factor vs Shear Displacement for Geotextile TS420

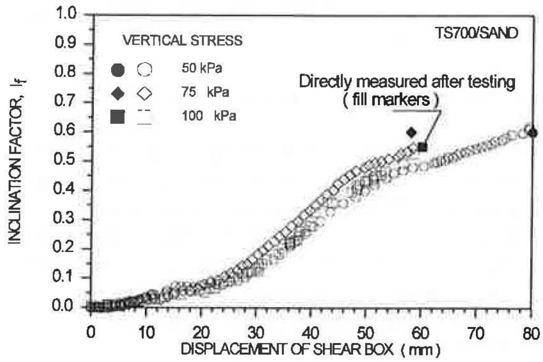

Fig. 8 Inclination Factor vs Shear Displacement for Geotextile TS700

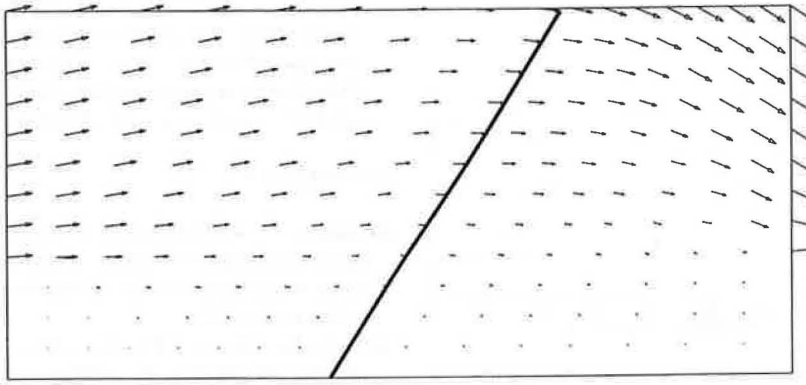

Fig. 9 Displacement Field for Reinforced Sample
at Shear Displacement of 35 mm

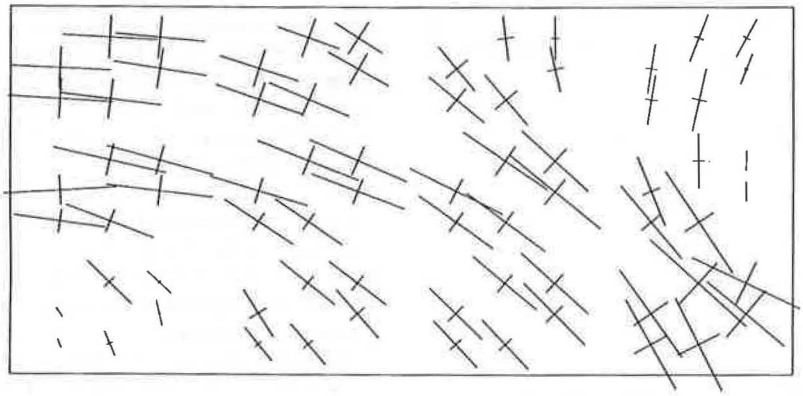

Fig. 10a Principal Stress Field of Unreinforced Soil

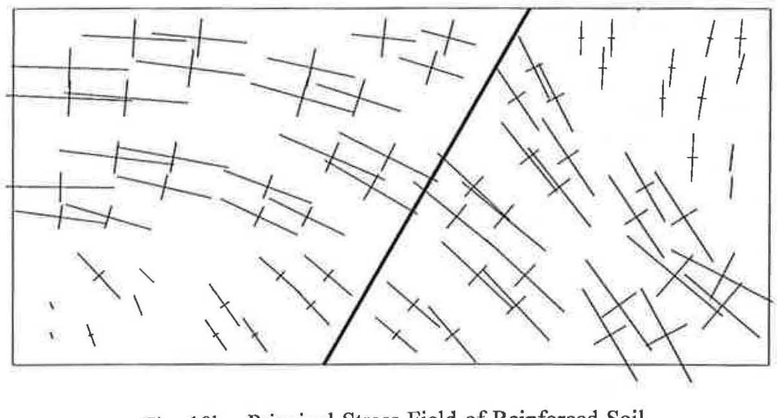

Fig. 10b Principal Stress Field of Reinforced Soil

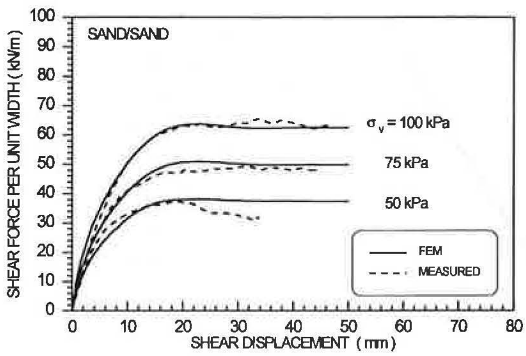

Fig. 11 Measured and FEM Calculated Results for Large Direct Shear of Unreinforced Sand

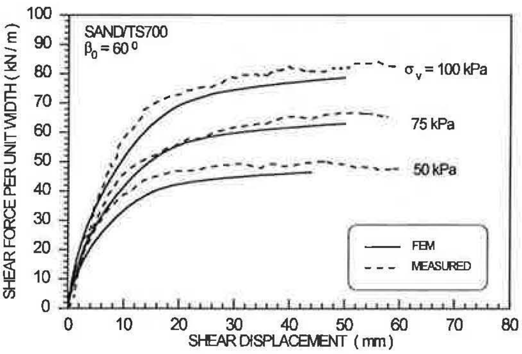

Fig. 12 Measured and FEM Calculated Results for Sand Reinforced by Geotextile TS700

4. CONCLUSIONS

Large direct shear model tests and finite element analysis have been conducted to investigate the mobilized strain and orientation of nonwoven, needle-punched geotextile reinforcement which were caused by the localized deformation of confining soil associated with the development of a shear surface. The main conclusions are as follows:

- The mobilized strain in the geotextile decreased with increasing geotextile stiffness. The limiting strains in geotextile associated with the peak shear strength of backfill soil have been found to be in the order of 5 % to 10 %.
- The orientation of geotextile reinforcement force seems independent on the geotextile stiffness. At shear displacement corresponding to the ultimate strength of soil, the values of inclination factor, I_β, are in the order of 0.25 to 0.50.
- The test method presented herein may be a realistic approach for determining the magnitude and orientation of the mobilized reinforcement force that is necessary in the stability analysis of geotextile reinforced earth structures.

REFERENCES

Bonaparte, R. & Christopher, B. R. (1987). Design and construction of reinforced embankments over weak foundation, *Transportation Research Record 1153*, pp. 26-39.

Delmas, Ph., Queyroi, D., Quaresma, M., De Saint Amand & Puech, A. (1992). Failure of an experimental embankment on soft soil reinforced with geotextile: Guiche. *Geotextiles, Geomembranes and Related Products*, ed. Den-Hoedt, Balkema, Rotterdam.

Fowler, J. (1982). Theoretical design considerations for fabric reinforced embankments. *Proc. 2nd Int. Conf. on Geotextiles*, Vol. 3, pp. 665-670.

Huisman, M.G.H. (1987). Design guideline for reinforced embankments on soft soils using Stabilenka reinforcing mats. *Enka Technical Report*, Arnhem.

Jewell, R.A. (1982). A limit equilibrium design method for reinforced embankments. Proc. *2nd Int.Conf. on Geotextiles*, Vol. 3. pp. 671-676.

Quast, P. (1983). Polyester reinforcing fabric mats for the improvement of the embankment stability. *Proc. 8th European Conf. on Soil Mechanics and Foundation Engineering*, Vol. 2, pp. 531-534.

Vermeer, P.A. and Brinkgreve, R.B.J. (1995). Finite element code for soil and rock analyses (eds). Balkema, Rotterdam.